

## Dark sequential $Z'$ portal: Collider and direct detection experiments

Giorgio Arcadi,<sup>1,†</sup> Miguel D. Campos,<sup>1,\*</sup> Manfred Lindner,<sup>1</sup> Antonio Masiero,<sup>2,3,‡</sup> and Farinaldo S. Queiroz<sup>1,4,§</sup>

<sup>1</sup>Max-Planck-Institut für Kernphysik, Saupfercheckweg 1, 69117 Heidelberg, Germany

<sup>2</sup>Dipartimento di Fisica e Astronomia “G. Galilei,” Università di Padova, I-35131 Padova, Italy

<sup>3</sup>Istituto Nazionale Fisica Nucleare, Sezione di Padova, I-35131 Padova, Italy

<sup>4</sup>International Institute of Physics, Federal University of Rio Grande do Norte, Campus Universitário, Lagoa Nova, Natal, Rio Grande do Norte 59078-970, Brazil



(Received 18 August 2017; published 13 February 2018)

We revisit the status of a Majorana fermion as a dark matter candidate when a sequential  $Z'$  gauge boson dictates the dark matter phenomenology. Direct dark matter detection signatures rise from dark matter-nucleus scatterings at bubble chamber and liquid xenon detectors, and from the flux of neutrinos from the Sun measured by the IceCube experiment, which is governed by the spin-dependent dark matter-nucleus scattering. On the collider side, LHC searches for *dilepton* and *monojet + missing energy* signals play an important role. The relic density and perturbativity requirements are also addressed. By exploiting the dark matter complementarity we outline the region of parameter space where one can successfully have a Majorana dark matter particle in light of current and planned experimental sensitivities.

DOI: [10.1103/PhysRevD.97.043009](https://doi.org/10.1103/PhysRevD.97.043009)

### I. INTRODUCTION

The existence of dark matter (DM) is a fact that has been accumulating evidence since the early 1970s (or even before if we consider the analysis done by Franz Zwicky in 1933 that led to him coining the term *Dunkle Materie* [1]). However its true nature remains an open question in physics as of today. Among the particle candidates, weakly interacting massive particles (WIMPs) stand out for being able to reproduce the observed relic abundance in a rather natural way and predict signals at current or planned experiments [2]. Despite this theoretical motivation and intense experimental efforts, the existence of WIMPs has not yet been established (for a recent review see [3]), for which distinct candidates and their possible signals in different detectors must be explored.

The experimental efforts can be roughly classified in three categories: indirect detection [4,5], direct detection (DD) [6–10] and collider searches [11–13], having each of these generally complementary characteristics. Although,

depending on the details of the model, the different search strategies are not equally effective. Indeed, in the scenario investigated here—Majorana fermion dark matter—indirect searches performed by experiments like Fermi-LAT, MAGIC and H.E.S.S. cannot probe the parameter space corresponding to the viable DM relic density [14–24]. Even with the Cherenkov Telescope Array, indirect detection probes are bound to be subdominant [25–30].<sup>1</sup> This is because the s-wave (i.e. velocity independent) component of its annihilation cross section into standard model (SM) fermions is helicity suppressed.<sup>2</sup> On the other hand, even if not influencing the flux of gamma rays/cosmic rays, DM annihilation processes occurring at present times can effectively influence the flux of neutrinos from the Sun, detectable by neutrino telescopes such as IceCube. This is due to the large exposure of these detectors to the Sun and, more importantly, because the neutrino flux is dictated by the unsuppressed WIMP-nucleon scattering cross section. For these reasons neutrinos from the Sun offer a complementary probe with respect to Earth-based experiments [33–38].

\* miguel.campos@mpi-hd.mpg.de

† arcadi@mpi-hd.mpg.de

‡ masiero@pd.infn.it

§ queiroz@mpi-hd.mpg.de

Published by the American Physical Society under the terms of the [Creative Commons Attribution 4.0 International license](https://creativecommons.org/licenses/by/4.0/). Further distribution of this work must maintain attribution to the author(s) and the published article's title, journal citation, and DOI. Funded by SCOAP<sup>3</sup>.

<sup>1</sup>It has been noted that Majorana particles mediated by a charged scalar can yield observable indirect detection signatures via internal bremsstrahlung, but this is not the scenario under study [31,32].

<sup>2</sup>Indirect detection can actually be an effective probe in some specific scenarios, like for example light DM annihilating into  $\bar{b}b$  or DM with dominant s-wave annihilations into gauge bosons. We do not consider these scenarios in this work.

In particular, we perform a detailed study of the phenomenology of a Majorana DM candidate interacting with a spin-1 mediator dubbed  $Z'$ . For simplicity, and to minimize the number of free parameters, we assume that the  $Z'$  couples with the SM fermions in the exact same way as the SM  $Z$  boson [39].<sup>3</sup> This setup is also referred to as the sequential standard model (SSM). Alternative assignments of these couplings can be motivated by identifying the  $Z'$  with the gauge boson of an additional, with respect to the SM gauge group,  $U(1)$  symmetry [56–68]. Given our assumptions, the model has only three free parameters, being the DM and  $Z'$  masses and the coupling of the DM with the  $Z'$ .

The important observables in this minimized setup are the dark matter relic density, the spin-dependent (SD) WIMP-nucleon scattering cross section, and the  $Z'$  production rate at the LHC. The dark matter relic density is computed in the usual thermal equilibrium framework leading to a freeze-out governed by the dark matter annihilation cross section into SM fermions. The direct dark matter detection signatures stem from spin-dependent dark matter-nucleus scatterings at the Bubble Chamber and Liquid Xenon detectors and from dark matter annihilations in the Sun. As for colliders, LHC searches for signal events in dilepton and monojet channels provide restrictive bounds on the model. Both probes are highly sensitive to the  $Z'$  production cross section at the LHC.

That said, we exploit the complementarity between these observables to outline the viable region of parameter where one can successfully have a Majorana dark matter particle in the context of the sequential dark  $Z'$  portal.<sup>4</sup>

Our work is organized as follows: in Sec. II we describe the Majorana dark matter model we investigate; in Sec. III we introduce the observables and experimental constraints; in Sec. IV we summarize and discuss our finding. Finally, in Sec. V we draw our conclusions.

## II. THE DARK SEQUENTIAL $Z'$ PORTAL

Seen usually as natural consequences of a symmetry breaking chain in grand unified theories (GUTs) [67] and many other extended gauge sectors [56,57,62,69–75],  $U(1)$  groups are ubiquitous in high energy physics model building for being the simplest continuous Abelian group available. The breaking down to the SM group typically leads to a massive gauge boson. If the SM Higgs doublet is not charged under the new  $U(1)$  group and the  $U(1)$  symmetry is spontaneously broken via a scalar singlet then there is no mass mixing between the  $Z$  and  $Z'$  gauge bosons

<sup>3</sup>For other constructions in the context of Majorana dark matter see [40–55].

<sup>4</sup>We emphasize that we are concerned just with the DM phenomenology, and we do not explore the possibilities or limitations of the additional  $U(1)$  symmetry and consider just the constraints coming from DM searches.

[76].<sup>5</sup> In this kind of framework the  $Z'$  represents the only “portal” between the DM and the SM fermions.<sup>6</sup> Spin-1 portals are also among the most adopted benchmarks for collider searches of dark matter. In this case, however, “simplified” models in which the  $Z'$  interacts only with quarks are customarily considered; see however [78]. These kinds of setups are contrived from the theoretical point of view [79,80] and do not account for the relevant impact of collider searches for dilepton resonances.

As a useful benchmark scenario, to describe the setup depicted above we consider the case of a Majorana fermion coupled with a sequential  $Z'$  boson, and then refer to it as the sequential dark  $Z'$  portal. The relevant part of the Lagrangian then looks like

$$\mathcal{L} \supset \left[ g_\chi \chi \gamma^\mu \gamma^5 \chi + \sum_{f \in \text{SM}} \bar{f} \gamma^\mu (g_{fv} + g_{fa} \gamma^5) f \right] Z'_\mu, \quad (2.1)$$

where the sum is over all the SM fermions and the factors  $g_{fv}$  and  $g_{fa}$  are given by

$$\begin{aligned} g_{uv} &= \frac{-e}{4} \left( \frac{5}{3} \tan \theta_w - \cot \theta_w \right), & g_{ua} &= \frac{-e}{4} (\tan \theta_w + \cot \theta_w) \\ g_{dv} &= \frac{e}{4} \left( \frac{1}{3} \tan \theta_w - \cot \theta_w \right), & g_{da} &= \frac{e}{4} (\tan \theta_w + \cot \theta_w) \\ g_{\ell v} &= \frac{e}{4} (3 \tan \theta_w - \cot \theta_w), & g_{\ell a} &= \frac{e}{4} (\tan \theta_w + \cot \theta_w) \\ g_{\nu v} &= \frac{e}{4} (\tan \theta_w + \cot \theta_w), & g_{\nu a} &= \frac{-e}{4} (\tan \theta_w + \cot \theta_w), \end{aligned} \quad (2.2)$$

where  $u$ ,  $d$ ,  $\ell$  and  $\nu$  are the up-type, down-type quarks, charged leptons and neutrinos respectively,  $e = \sqrt{4\pi\alpha}$  is the electromagnetic coupling and  $\theta_w$  is the Weinberg angle. We highlight that it is nontrivial to construct a UV complete realization of this sequential  $Z'$  portal. It is hard to build an anomaly-free model in which the  $Z'$  interactions with SM particles mimic precisely those from the SM  $Z$  boson.

<sup>5</sup>In this kind of setup (tree-level) mixing between the  $Z$  and the  $Z'$  is absent only if the charges of the SM fermions under the new symmetry are proportional to  $B - L$  [77], not the case considered here, since, otherwise, a nonzero charge for the SM Higgs is required by anomaly cancellation. This requirement might be relaxed in more complicated constructions [76]. The purpose of this paper is a phenomenological study without referring to specific UV frameworks. Theoretical aspects related to possible UV completions are nevertheless briefly discussed in Sec. IV.

<sup>6</sup>We consider the case in which the  $Z'$  has direct coupling with the SM fermions; i.e. SM fermions are charged under the hypothetical new  $U(1)$  symmetry. Alternatively, a coupling between the  $Z'$  and the SM can be originated by the Lorentz and gauge invariant kinetic mixing term  $\delta B^{\mu\nu} B'_{\mu\nu}$ . We do not consider here this kind of scenario. As pointed in the last section it is nevertheless possible to straightforwardly generalize our results.

Nevertheless, we emphasize that we remain agnostic about the origin of such a sequential  $Z'$  model and focus on the phenomenological aspects.

The Lagrangian in Eq. (2.1) generates two kind of operators relevant for direct detection of DM:  $\bar{f}\gamma^\mu f\chi\gamma_\mu\gamma_5\chi$  and  $\bar{f}\gamma^\mu\gamma_5 f\chi\gamma_\mu\gamma_5\chi$ . The former yields a spin-independent (SI) interaction, whereas the latter yields a SD interaction. Since the SI cross section is velocity suppressed (being the scattering cross section proportional to  $v^2 \sim 10^{-6}$ ) we concentrate on the constraints coming exclusively from SD searches.

Now that we have set up the framework to investigate, we discuss the relevant observables and respective constraints applicable to the model.

### III. EXPERIMENTAL CONSTRAINTS

#### A. Relic density

The first requirement that we impose upon the framework presented is that the Majorana fermion reproduces the

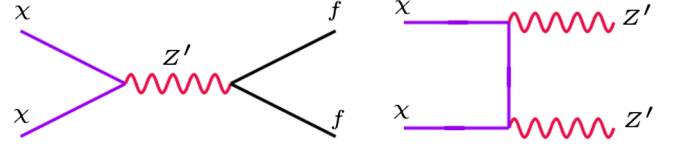


FIG. 1. Feynman diagrams relevant for dark matter annihilation. The first encompasses all possible annihilations into SM particles through the  $Z'$  portal, whereas the second encompasses the self-annihilation into  $Z'$  gauge bosons.

observed relic abundance of DM, namely  $\Omega h^2 \approx 0.12$  [81] through thermal production. The annihilation channels relevant for this production are presented in Fig. 1 and correspond to an s-channel annihilation mediated by a  $Z'$  and a t-channel process  $\chi\chi \rightarrow Z'Z'$  when kinematically allowed.

The DM relic density has been precisely determined in a numerical way through the package `MicrOmEGAS 4.3.2` [82]. Useful analytical approximations are nevertheless provided by the velocity expansion (see also [66]),

$$\begin{aligned} \langle\sigma v\rangle_{ff} &= \sum_f n_c^f \frac{2\sqrt{m_\chi^2 - m_f^2}}{\pi m_\chi M_{Z'}^4 (M_{Z'}^2 - 4m_\chi^2)^2} [(g_{fa})^2 g_\chi^2 m_f^2 (M_{Z'}^2 - 4m_\chi^2)^2] \\ &\quad - \frac{v^2}{6\pi m_\chi M_{Z'}^4 \sqrt{m_\chi^2 - m_f^2} (M_{Z'}^2 - 4m_\chi^2)^3} [(g_{fa})^2 \{-g_\chi^2 (M_{Z'}^2 - 4m_\chi^2) \\ &\quad \times (23m_f^4 M_{Z'}^4 - 192m_f^2 m_\chi^6 - 4m_f^2 m_\chi^2 M_{Z'}^2 (30m_f^2 + 7M_{Z'}^2) \\ &\quad + 8m_\chi^4 (30m_f^4 + 12m_f^2 M_{Z'}^2 + M_{Z'}^4))\} \\ &\quad + M_{Z'}^4 (g_{fv})^2 \{4g_\chi^2 (m_f^4 + m_f^2 m_\chi^2 - 2m_\chi^4) (M_{Z'}^2 - 4m_\chi^2)\}]; \end{aligned} \quad (3.1)$$

$$\begin{aligned} \langle\sigma v\rangle_{Z'Z'} &= \frac{g_\chi^4}{\pi m_\chi^2} \left(1 - \frac{M_{Z'}^2}{m_\chi^2}\right)^{\frac{3}{2}} \left(1 - \frac{M_{Z'}^2}{2m_\chi^2}\right)^{-2} \\ &\quad + \frac{g_\chi^4 v^2}{3\pi m_\chi^2} \sqrt{1 - \frac{M_{Z'}^2}{m_\chi^2}} \left(1 - \frac{M_{Z'}^2}{2m_\chi^2}\right)^{-4} \left(\frac{23}{16} \frac{M_{Z'}^6}{m_\chi^6} - \frac{59}{8} \frac{M_{Z'}^4}{m_\chi^4} + \frac{43}{4} \frac{M_{Z'}^2}{m_\chi^2} + 2 - 12 \frac{m_\chi^2}{M_{Z'}^2} + 8 \frac{m_\chi^4}{M_{Z'}^4}\right), \end{aligned} \quad (3.2)$$

where  $n_c^f$  is the color factor and the  $g_{fv}, g_{fa}, f = u, d, e, \mu, \tau, \nu$  have been defined in Eq. (2.2). In the first expression the sum runs over the final states kinematically accessible for a given value of the DM mass  $m_\chi$ .

Some important features are worth noticing in the expressions above. Concerning the annihilation into fermions we see that the s-wave (velocity independent term) is proportional to  $\frac{m_f^2}{M_{Z'}^4}$  with  $m_f$  being the final state fermion mass. Hence, unless annihilation into top quarks is kinematically accessible, the s-wave term of the DM annihilation cross section is strongly suppressed so that the

dominant contribution comes from the p-wave term that does exhibit the  $Z'$  resonance. Because of this, there is a strong mismatch between the value of the annihilation cross section at thermal freeze-out, relevant for the relic density, corresponding to  $v \sim 0.3$ , and the one at present times, possibly relevant for an indirect detection signal, corresponding instead to  $v \sim 10^{-3}$ .

The reasoning above explains why indirect dark matter detection is bound to be subdominant in this scenario. Because of the helicity suppression of the s-wave component, the thermally favored value of the DM annihilation cross section at chemical freeze-out would correspond to

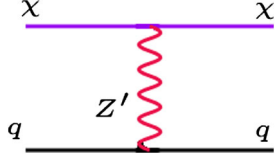


FIG. 2. Feynman diagram relevant for direct detection. The dark matter scattering off nucleons occurs via the  $Z'$  t-channel exchange.

a suppressed annihilation at present times. Comparable values for the annihilation cross section at freeze-out and at present times could be achieved for  $m_\chi \gtrsim m_{\text{top}}$ , when  $m_\chi \simeq 200$  GeV. However indirect detection limits cannot yet strongly probe thermal dark matter in this mass range. We remind the reader that such helicity suppression of the annihilation cross section is not present in the case of a Dirac fermion [39,57].

When the dark matter mass becomes larger than the  $Z'$  mass the annihilation to  $Z'$  pairs opens up, and Eq. (3.2) becomes relevant. Notice that Eq. (3.2) features s-wave and p-wave contributions. The s-wave term scales with  $1/m_\chi^2$ , so one can naively expect that this contribution is small since we are dealing with a heavy DM particle, with the  $m_\chi > M_{Z'}$  term. However, the p-wave term grows with  $m_\chi^2/M_{Z'}^4$ . Since we are now focused on a heavy DM particle, this enhancement with  $m_\chi^2$  compensates the  $v^2$  suppression and dominates the overall DM annihilation. Such enhancement with  $m_\chi^2/M_{Z'}^4$  is related to the annihilation into longitudinal  $Z'$  pairs and is actually pathological, due to the non-UV complete framework we investigate. We discuss this point in further detail in Sec. III D.

## B. Direct detection

DD signatures of the model rely on the SD dark matter scattering off nucleons via the t-channel  $Z'$  exchange as displayed in Fig. 2. It is dictated by the axial couplings  $g_{fa}$  defined in Eq. (2.2), and described by the following cross section,

$$\sigma_{\chi N}^{\text{SD}} = \frac{12\mu_{\chi p}^2 g_\chi^2}{\pi M_{Z'}^4} [g_{ua}\Delta_u^N + g_{da}(\Delta_d^N + \Delta_s^N)]^2, \quad N = p, n. \quad (3.3)$$

Sizeable SI interactions are, on the contrary, absent since Majorana fermions have null vectorial couplings. As evident from Eq. (3.3) the ratio between the scattering cross sections on the proton and neutron depends essentially on the combination of the couplings  $g_{(u,d)a}$  and of the parameters  $\Delta_{u,d,s}^N$  and it is then constant. For the model under consideration we have that  $\sigma_{\chi n}^{\text{SD}}/\sigma_{\chi p}^{\text{SD}} \approx 0.76$ . Despite the presence of DM scattering on protons and neutrons, DD experiments have typically very different sensitivities to the two cross sections. The sensitivity of target material to DM

spin dependent interactions depends on the presence of an unpaired nucleon in its atom. A given target material has much better sensitivity to SD interactions on protons,  $SD_p$  (neutrons,  $SD_n$ ), in case the unpaired nucleon is a proton (neutron). For this reason we present, in this work, bounds and projected sensitivities both from the PICO experiment, whose target material,  $C_3F_8$ , features an unpaired proton, and from LUX and XENON1T, which are xenon-based experiments and thus better suited to probe SD interactions between DM and neutrons. The different bounds are individually discussed in more detail in the following subsections.

### 1. Spin-dependent scattering off protons

The bubble chamber PICO-60 detector sets the strongest limits on  $SD_p$ . These are based on an exposure of 1167 kg · days of data taken between November 2016 and January 2017 and exclude  $SD_p$  of  $3.4 \times 10^{-41}$  cm<sup>2</sup> for a 30 GeV DM mass [83]. One should notice that the limits presented by the PICO collaboration cover values of the DM mass only up to 1 TeV. Since we have considered, in our study, a broader mass range for the DM we have used an extrapolation. This operation is reliable since for heavy DM masses the scattering rate scales linearly with the number density of DM particles.<sup>7</sup>

Dark matter scattering off nuclei is not only tested in underground facilities. Searches of neutrino fluxes coming from annihilations of DM particles captured in the Sun can represent a complementary probe (see e.g. [38]). We recall indeed that the flux of neutrinos observed from the Sun is connected to the DM capture and annihilation rate at the Sun. The capture rate is mostly governed by the DM scattering off hydrogen, helium and oxygen, while the destruction rate is instead governed by the annihilation cross section in the  $v \rightarrow 0$  limit. In the case in which the equilibrium condition between the capture and destruction rate is met, it is possible to get rid of the dependence of the neutrino flux on the annihilation cross section and cast limits in terms of the SD cross section only. The equilibrium condition can be satisfied for values of the annihilation cross section much below the thermal value as long as the SD scattering cross section is sufficiently large. For this reason the model under study can be efficiently tested by neutrino telescopes while the typical values of the DM annihilation cross section are not accessible to conventional indirect detection strategies. A residual dependence on the

<sup>7</sup>In reality, xenon detectors are also sensitive to SD scattering off protons. This is because the even numbers of proton in the xenon isotopes do not perfectly cancel each other's spin, giving rise to a small net spin. Such small net spin explains why xenon-based detectors provide relatively much weaker limits on the SD dark matter scattering off protons. The current and projected limits from the XENON1T experiment have been obtained but they are substantially weaker than PICO's and therefore were not considered further.

annihilation cross section is nevertheless present since the neutrino flux actually depends on the type of annihilation final states since they induce distinct neutrino yields, and consequently different limits on the SD cross section according to the dominant annihilation channel of the DM. This effect has been taken into account in our study. For concreteness the DM capture rate at the Sun can be written as [84]

$$C_{\text{DM}} = 10^{20} \text{ s}^{-1} \left( \frac{1 \text{ TeV}}{m_\chi} \right)^2 \frac{2.77\sigma_{SD_p} + 4270\sigma_{SI_p}}{10^{-40} \text{ cm}^2} \quad (3.4)$$

for DM masses above 1 TeV.

From Eq. (3.4) one can see that the nonobservation of a neutrino signal from the Sun can yield limits on both the SD and SI scattering cross sections. The bounds on the SI are stronger due to larger overall factor in Eq. (3.4). Currently IceCube imposes  $SD_p < 10^{-40} \text{ cm}^2$  and  $SI_p < 10^{-43} \text{ cm}^2$  for a 100 GeV DM mass, annihilating into WW [85]. Direct detection experiments such as XENON, LUX and PANDA-X provide however limits below  $10^{-45} \text{ cm}^2$  on the SI scattering cross section [86–90], while PICO sets  $SD_p < 4 \times 10^{-41} \text{ cm}^2$  [83]. Because of this, IceCube searches for DM annihilations in the Sun are only truly relevant when it comes to  $SD_p$  scattering. In the example above we used IceCube limits for DM annihilations into WW gauge bosons, but if we had adopted the bounds for annihilations into  $\tau\tau$  which yield a harder neutrino spectrum, then IceCube limits can indeed be better than the ones stemming from PICO, excluding  $SD_p = 2 \times 10^{-41} \text{ cm}^2$ . Therefore, keep in mind that the limits coming from the IceCube detector appearing in Figs. 4–6 are based on the SD dark matter scattering off protons.

We now discuss the bounds based on SD scatterings off neutrons.

## 2. Spin-dependent scattering off neutrons

As aforementioned the presence of an unpaired neutron in xenon isotopes makes xenon-based detectors such as PANDA-X, LUX and XENON1T experiments the most sensitive to such nuclear recoil interactions.

The LUX collaboration has recently placed new limits on  $SD_n$  using 129.5 kg-year exposure, excluding  $SD_n = 1.6 \times 10^{-41} \text{ cm}^2$  for a 35 GeV DM mass [91]. These new bounds slightly improve the limit placed by the PANDA-X collaboration [87]. This LUX limit is represented by a dashed green line.

As for the projected sensitivity on  $SD_n$  we adopted as baseline the XENON100 results. Since the XENON1T collaboration expects to achieve a 2 orders of magnitude improvement on the SI cross section with 2 year  $\times$  ton exposure over the previous XENON100 result, we assumed the same rescaling for the SD scattering cross section [92]. In other words, since the XENON1T projected limit with

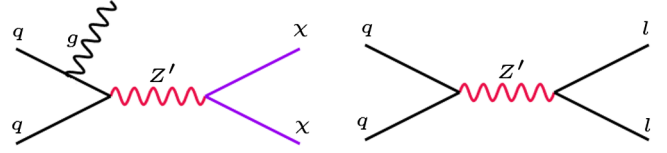


FIG. 3. Feynman diagrams relevant for collider probes. The first diagram represents monojet searches for dark matter, where the  $Z'$  decays invisibly with a jet being radiated from the initial state. The second accounts for the resonance production of the  $Z'$  gauge boson. The latter is not particularly sensitive to dark matter, but it strongly restricts the  $Z'$  mass with great impact to this particular model.

full exposure is expected to improve its predecessor by a factor of 100 concerning spin-independent scattering, we use this same 100 factor to project its sensitivity to spin-dependent DM-neutron scattering.

Now that we have described the experimental searches for spin-dependent DM-nucleon scattering we remark on some key theoretical ingredients having in mind Eqs. (3.1) to (3.3).

(i) The scattering cross section off nucleons scales with  $Z'$  mass to the fourth power. Since we fix the  $g_\chi$  coupling to different values, the direct detection limits based on this scattering cross section are simply straight lines in the log-log scale plots as shown in Figs. 4–6.<sup>8</sup>

(ii) Since we have a sequential  $Z'$  gauge boson,  $|g_{ua}| = |g_{da}|$ , there is essentially no theoretical bias toward scattering off proton or neutrons.

(iii) PICO, LUX and XENON1T experimental sensitivities to our model rely only on the experimental parameters  $\Delta_u^N$ ,  $\Delta_d^N$  and  $\Delta_s^N$ .

(iv) The annihilation into SM fermions might favor a particular final state depending on the DM mass, due to kinematic effects. These threshold effects are visible near the top quark and the  $Z'$  mass. These channels have a significant impact on the annihilation cross section. These two effects explain the wavy behavior of the IceCube limits exhibited in Figs. 4–6.

## C. Colliders

Since we are discussing a model in the context of vector mediators, it is well known that the most efficient way to probe this simplified dark matter model is through the monojet and dilepton data sets [39] (see Fig. 3 for a schematic representation of the Feynman diagrams of the

<sup>8</sup>This implicitly assumes that in computing the event rate measured in DD experiments, the experimentally determined local DM density is adopted, implying that the fermionic DM candidate is assumed to account for the total DM component of the Universe and to have the correct relic density irrespective of the values of the parameters of the theory. Outside the isocontours corresponding to conventional thermal production (see Figs. 4–6) we implicitly assume that the correct DM relic density is accounted by nonthermal production and/or modified cosmology [93–95].

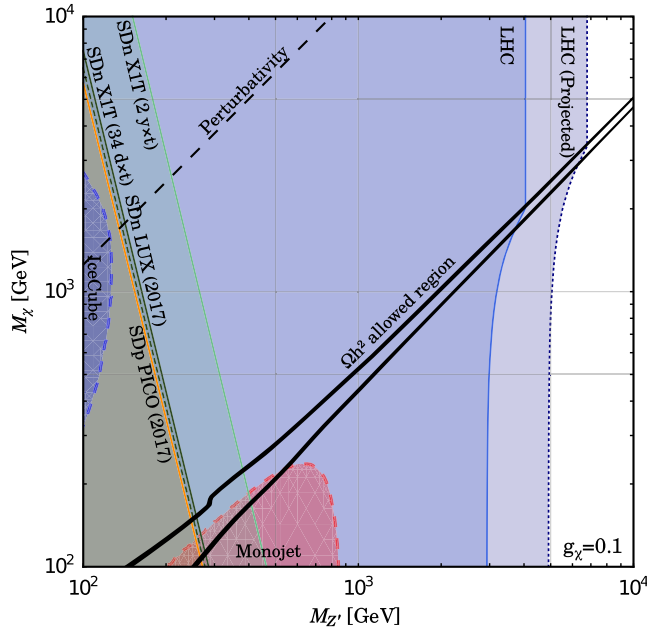


FIG. 4. Summary plot for  $g_\chi = 0.1$ . The solid black curve outlines the region of parameter space with the correct relic density. From left to right, in dashed blue is the parameter space excluded by IceCube; the orange solid line represents the current bound from PICO, the dashed green line the current bound from LUX on SD scattering off neutrons with 129.5 kg-year exposure, and the solid green line the projected bound from XENON1T on SD scattering off neutrons with 34 d  $\times$  t of exposure; further right in light green, we show the projected sensitivity from XENON1T on SD scattering off neutrons with 2 y  $\times$  t exposure; the upper region inside the dashed black line delimits the nonperturbative regime; the dashed red curve exhibits the parameter space excluded by the LHC based on monojet data; solid (dotted) blue vertical lines delimit the current (projected) LHC exclusion regions derived from dilepton data.

relevant processes), the latter providing the most restrictive limits.

The limits we included were derived from the LHC searches for the sequential SM  $Z'$  decaying into charged leptons [96] with an integrated luminosity of 36.1 fb $^{-1}$  and 13 TeV center-of-mass energy. They rely on the fact that a heavy spin-1 additional boson  $Z'$  would decay producing a narrow resonance in the dilepton channel that has a low and well-understood background. Subsequently an upper limit on the cross section times the branching ratio can be extracted, and consequently a lower bound on the  $Z'$  mass can be derived. Two limits are often quoted, one based on the dielectron data (4.3 TeV) and another on the dimuon data (4 TeV). The dielectron channel yields a slightly stronger limit than the dimuon one due to the larger acceptance/efficiency [96]. The sequential  $Z'$  boson features a fairly large decay width and therefore the bound on the  $Z'$  mass is subject to sizable uncertainties. For instance, in the combined channel (dielectron + dimuon) the lower mass bound on the  $Z'$  ranges from 4.3 to 4.8 TeV (see Fig. 4

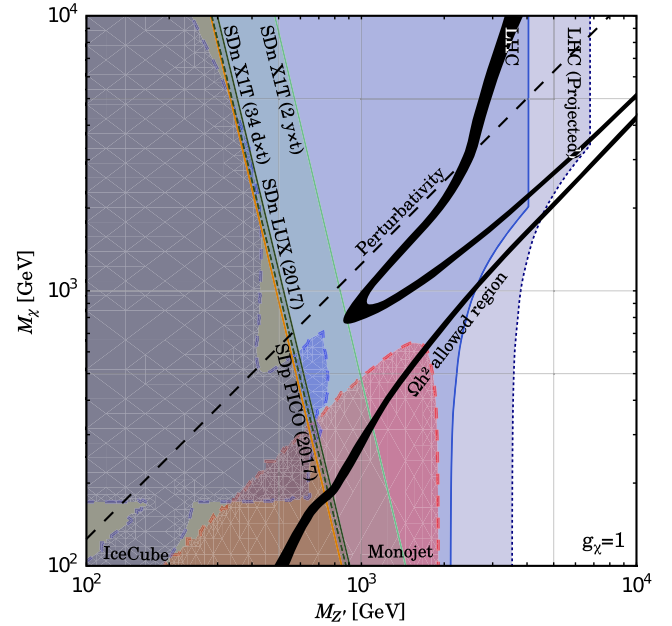


FIG. 5. Exclusion limits for  $g_\chi = 1$ . The solid black curve outlines the region of parameter space with the correct relic density. From left to right, in dashed blue is the parameter space excluded by IceCube; the orange solid line represents the current bound from PICO, the dashed green line the current bound from LUX on SD scattering off neutrons with 129.5 kg-year exposure, and the solid green line the projected bound from XENON1T on SD scattering off neutrons with 34 d  $\times$  t of exposure; further right in light green, we show the projected sensitivity from XENON1T on SD scattering off neutrons with 2 y  $\times$  t exposure; the upper region inside the dashed black line delimits the nonperturbative regime; the dashed red curve exhibits the parameter space excluded by the LHC based on monojet data; solid (dotted) blue vertical lines delimit the current (projected) LHC exclusion regions derived from dilepton data.

of [96]). Moreover, there are also mild systematic uncertainties associated to dilepton resonant searches [97]. In light of that, we decided to take a conservative approach and adopted the LHC limit obtained using the dimuon channel, which imposes  $M_{Z'} > 4$  TeV. Despite applying the limit on the  $Z'$  mass based on dimuon data only, we refer to this collider bound as dilepton hereafter. This limit is represented by a solid vertical line in Figs. 4 and 5. In Fig. 6 this limit is shown with a dot-dashed line instead because here we adopted  $g_\chi = 4\pi$ , which is large enough to potentially alter the total  $Z'$  width, beyond the narrow width approximation used to derive the LHC bound. Therefore, this limit should be applied with care. A dedicated collider study of the  $Z'$  width in the sequential  $Z'$  model was performed elsewhere [96] and it lies outside the scope of the current work. According to [96], the deviations on the lower mass limit for  $Z'$  masses below 4 TeV are mild.

Keeping that in mind, we also include the projected bound, under the null result hypothesis for center-of-mass energy of

14 TeV and integrated luminosity of  $1000 \text{ fb}^{-1}$ ,<sup>9</sup> as a dotted blue line in Figs. 4–6, that would rule out the region  $M_{Z'} \approx 6.7 \text{ TeV}$ . We emphasize that the LHC bounds for large values of  $g_\chi$  may not be considered at face value since for large couplings the narrow width approximation fails.

Anyways, as one clearly sees, the exclusion limits in Figs. 4–6, from searches of dilepton resonances,

become weaker in the lower portion of the plots, i.e. when the DM is lighter than the  $Z'$ . Indeed the analysis from the ATLAS experiment incorporates only decay channels into SM states for the  $Z'$ . This does not occur in our case when  $2m_\chi < M_{Z'}$ . The total decay width of the  $Z'$  gets indeed modified as [98]

$$\begin{aligned} \Gamma_{Z'} &= \sum_{f \in \text{SM}} \theta(M_{Z'} - 2m_f) \frac{n_c M_{Z'}}{12\pi} \sqrt{1 - \frac{4m_f^2}{M_{Z'}^2}} \left[ g_{fv}^2 \left( 1 + \frac{2m_f^2}{M_{Z'}^2} \right) + g_{fa}^2 \left( 1 - \frac{4m_f^2}{M_{Z'}^2} \right) \right] \\ &\times \theta(M_{Z'} - 2m_\chi) \frac{M_{Z'}}{12\pi} \sqrt{1 - \frac{4m_\chi^2}{M_{Z'}^2}} g_\chi^2 \left( 1 - \frac{4m_\chi^2}{M_{Z'}^2} \right), \end{aligned} \quad (3.5)$$

where  $g_{fv}$  and  $g_{fa}$  were given in Eq. (2.2) and  $\theta$  is the unit step function. Consequently, the branching ratio to dilepton becomes in this regime

$$\begin{aligned} \frac{\Gamma(Z' \rightarrow \ell\ell)}{\Gamma(Z' \rightarrow ff)} &\Rightarrow \frac{\Gamma(Z' \rightarrow \ell\ell)}{\Gamma(Z' \rightarrow ff) + \Gamma(Z' \rightarrow \chi\chi)} \\ &= \frac{\Gamma(Z' \rightarrow \ell\ell)}{\Gamma(Z' \rightarrow ff)} (1 - \text{Br}(Z' \rightarrow \chi\chi)) = \text{Br}(Z'_{\text{SSM}} \rightarrow \ell\ell) [1 - \text{Br}(Z' \rightarrow \chi\chi)], \end{aligned} \quad (3.6)$$

where  $f$  is a SM fermion.

Therefore, the exclusion limit on the  $Z'$  mass which depends linearly on  $\text{Br}(Z'_{\text{SSM}} \rightarrow \ell\ell)$  is weakened by  $[1 - \text{Br}(Z' \rightarrow \chi\chi)]$ . Obviously, this effect takes place only when the decay of the  $Z'$  into DM pairs is kinematically accessible, as aforementioned. As can be easily argued the effect of opening the invisible decay channel is more prominent at the highest values of the coupling  $g_\chi$  since they correspond to higher values of the  $Z'$  invisible branching fraction.

The monojet bound features a complementary behavior with respect to the dilepton one. It is indeed based on searches of monojet events plus missing energy whose production rate is maximal when the  $Z'$  decay on shell mostly on DM pairs. For this reason the strongest bound is obtained for  $g_\chi = 4\pi$  and  $m_\chi < M_{Z'}/2$ . On the contrary, the size of the excluded region is increasingly reduced as  $g_\chi$  decreases and substantially no bound is present for  $m_\chi > M_{Z'}/2$ .

#### D. Perturbativity

As already discussed, the annihilation cross section associated to the  $\chi\chi \rightarrow Z'Z'$  process shows a rather peculiar behavior: it scales as  $m_\chi^2/M_{Z'}^4 v^2$  for  $m_\chi \gg M_{Z'}$  and hence it increases indefinitely with the value of the DM mass.

As discussed in [79,99] this is due to the longitudinal degrees of freedom of the  $Z'$  which induce a contribution in the annihilation amplitude proportional to  $\sqrt{s}m_\chi/M_{Z'}^2$ . (The annihilation into longitudinal degrees of freedom would actually induce a  $s/M_{Z'}^2$  scaling. The dependence on  $s$  is weakened because of cancellation between  $t$ - and  $u$ -channel diagrams [79].) The behavior of the annihilation cross section is, at this point, easily understood once we remember that for the relic density only the nonrelativistic limit,  $s \sim 4m_\chi^2$ , is relevant. The fact that the contribution associated to the annihilation into a longitudinal  $Z'$  pair appears in the p-wave term of velocity expansion can be inferred through  $CP$  and angular momentum conservation arguments [100]. As it is widely known, amplitudes increasing with the center-of-mass energy are pathological and violate perturbative unitarity at relatively low energy. The presence of a unitarity violating cross section is caused by the fact that we are considering a non-UV complete framework. In  $Z'$  models based on the spontaneous breaking of extra gauge symmetries the annihilation rate into  $Z'Z'$  is cured once the diagram with  $s$ -channel exchange of the scalar field responsible for the spontaneous breaking of the new theory is accounted for. (See e.g. [101]. Discussions on similar lines can be found also in [102,103].)

Since we do not rely on a UV complete model, we require that the amplitude of the process  $\chi\chi \rightarrow Z'Z'$  does not violate unitarity, in the same fashion as [79]. This requirement is translated in the following constraint:

<sup>9</sup><http://collider-reach.web.cern.ch/?rts1=13&lumi1=3.2&rts2=13&lumi2=13.3&pdf=MSTW2008nnlo68cl.LHgrid>

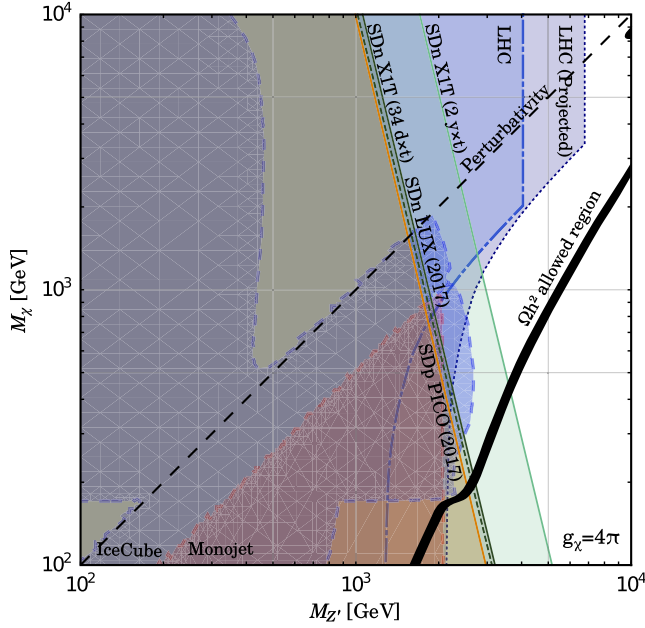


FIG. 6. Exclusion limits for  $g_\chi = 4\pi$ . The solid back curve outlines the region of parameter space with the correct relic density. From left to right, in dashed blue is the parameter space excluded by IceCube; the orange solid line represents the current bound from PICO, the dashed green line the current bound from LUX on SD scattering off neutrons with 129.5 kg-year exposure, and the solid green line the projected bound from XENON1T on SD scattering off neutrons with 34 d  $\times$  t of exposure; further right in light green, we show the projected sensitivity from XENON1T on SD scattering off neutrons with 2 y  $\times$  t exposure; the upper region inside the dashed black line delimits the nonperturbative regime; the dashed red curve exhibits the parameter space excluded by the LHC based on monojet data; dot-dashed (dotted) blue vertical lines delimit the current (projected) LHC exclusion regions derived from dilepton data.

$$\sqrt{s} < \frac{\pi M_{Z'}}{g_\chi^2 M_\chi}, \quad (3.7)$$

which can be expressed, in the nonrelativistic limit relevant for the DM relic density, as

$$M_\chi < \sqrt{\frac{\pi M_{Z'}}{2g_\chi^2}}. \quad (3.8)$$

We emphasize that Eq. (3.8) should be interpreted as a limit for the validity of the computations presented in this work. Beyond the region of parameter space delimited by Eq. (3.8) one should explicitly take into account additional degrees of freedom needed to unitarize the theory.

This condition excludes the region of parameter space in Figs. 4–6 above the dashed black line labeled as perturbativity in the figures. Now that we have described all observables of the simplified Majorana dark matter model, we gather all the ingredients and comment on our findings.

## IV. RESULTS

Our main results are summarized in Figs. 4–6 in the bidimensional plane  $M_{Z'}, m_\chi$  for three fixed values of  $g_\chi$ , i.e. 0.1, 1 and  $4\pi$  respectively. In the plots the parameter space accounting for the correct DM relic density is compared with the limits from the most relevant dark matter observables taking into account current and future experimental sensitivities to outline the region where one can have a viable Majorana fermion as dark matter. The individual origin of the different bounds reported in the plot has been discussed in the previous sections. Here we discuss more extensively the effect of their combination and the impact on the parameter space.

We start by commenting on the relic density. The correct DM relic density is represented, in Figs. 4–6, by black isocontours. For the lowest assignment of  $g_\chi$ , namely 0.1, the correct relic density is achieved only through resonantly enhanced, for  $m_\chi \sim M_{Z'}/2$ , annihilation into SM fermions. At  $g_\chi = 1$  the correct relic density is also easily achieved, for  $m_\chi > M_{Z'}$  through the  $\chi\chi \rightarrow Z'Z'$  annihilation process, and also a bit far from the resonance, when annihilations into  $\bar{t}t$  are maximally efficient. A large part of the viable parameter space for  $m_\chi > M_{Z'}$  is, however, excluded by the unitarity constraint. For  $g_\chi = 4\pi$  finally, the annihilation into  $Z'Z'$  is too efficient, always leading to underabundant DM, and the correct relic density is achieved through annihilations into SM fermions far from the  $m_\chi \sim M_{Z'}/2$  pole region.

Concerning the LHC, for fixed values of the couplings, the limits from searches of dilepton resonances, as long as  $M_{Z'} < 2m_\chi$ , are basically turned into an exclusion in the mass of the  $Z'$  independent on the value of  $g_\chi$ . On the contrary, when  $M_{Z'} > 2m_\chi$  the excluded value of  $M_{Z'}$  suffers the rescaling effect, described before, attributed to the invisible branching fraction of the  $Z'$  and actually depends on  $m_\chi$  and  $g_\chi$ . For  $g_\chi = 4\pi$  the exclusion bound can be reduced to 1 TeV<sup>10</sup> while for  $g_\chi = 0.1$ , the effect of the invisible branching ratio is, instead, marginal.

Generally speaking the bound from dilepton searches is the strongest for the kind of scenario under consideration (see also [67] for a dedicated study). The only exception is represented by the extreme assignment  $g_\chi = 4\pi$  for which, in the region  $m_\chi < M_{Z'}/2$ , DM direct detection poses the most competitive constraints. While in principle complementary to searches of dilepton resonances, searches for monojet events are not yet competitive with respect to other

<sup>10</sup>Notice that in this context one should consider a complementary bound from LEP [104] coming from eventual modifications of the dielectron production cross section. This kind of search tests the off-shell production of the  $Z'$  and then the limits depend only on its mass and coupling with the electrons, irrespective of the presence of other couplings. For the sequential  $Z'$  the limit is of approximately 1.8 TeV. For simplicity we have not reported the corresponding line in the plots. See however [3].

observational constraints. The reason mostly lies in the larger SM backgrounds which plague monojet searches with respect to the ones of lepton final states.

The sensitivity of this kind of experimental search receives a substantial improvement from XENON1T. Constraints by IceCube demonstrate a potentially good complementarity. They are however strongly dependent by the kind of annihilation final state of the DM. In the model considered they are mostly effective in the intermediate mass range of both the  $Z'$  and the DM, where the latter dominantly annihilates into  $\bar{t}t$ .

As emphasized, our findings are valid in the context of the sequential  $Z'$  model. However, since the direct detection limits scale with  $g_\chi^2 g_{fa}^2$  as well as the annihilation rate into SM fermions, and the dilepton bounds roughly scale up with  $g_{fv}^2$ , one can recast these findings to many Majorana fermion dark matter models. Dilepton bounds, as already noticed, represent the dominant constraint for the scenario under scrutiny. These bounds are basically determined by the size of the coupling of the  $Z'$  with the leptons so one might wonder about their model dependence. As it can be easily seen, the collider bound on the mass of the  $Z'$  would be weakened by reducing the size of the couplings  $g_{ve}$  and  $g_{ae}$  negligibly affecting the constraints from monojet, relic density, and DM searches, since the latter mostly rely on the couplings of the  $Z'$  with the DM and the quarks. However, a very strong suppression of the decay branching fraction of the  $Z'$  into leptons would imply that the limits from dilepton resonance searches should be replaced by the ones from searches of dijet resonances. For a sequential  $Z'$  similar sensitivities for dilepton and dijet searches would be achieved by rescaling the coupling of the  $Z'$  with the leptons by, approximately, a factor 0.03. In this case one should consider the recent analysis [105,106], for dijet searches, which excludes, assuming no invisible branching fraction, masses of the  $Z'$  between 2.5 and 3 TeV.<sup>11</sup> As it can be seen from Figs. 4–6 collider bounds would remain more competitive with respect to the ones from DM searches, as long as  $g_\chi \lesssim 1$ .

As shown in the previous section, the absence of UV completion poses problems of consistency which might impact the viable DM parameter space as efficiently as experimental constraints. One might then ask whether further phenomenological consequences should be expected once facing a consistent completion of the scenario under study. As already pointed out, the most straightforward theoretical embedding of the simplified model, analyzed in this work, would consist in identifying the  $Z'$  as the gauge bosons of a new, spontaneously broken,  $U(1)$  gauge group. In this case a fundamental requirement,

<sup>11</sup>These limits mostly refer to a simplified case in which the  $Z'$  features only vectorial or axial-vectorial flavor universal couplings with the SM quarks. They should be then intended as qualitative estimates for the case under study.

for a theoretically consistent model, is represented by the absence of anomalies. In the absence of beyond the standard model states a sequential  $U(1)'$  would be, “by construction,” anomaly free since the charges of the SM fermions under the new symmetry are the same as the SM hypercharge. This is not anymore the case once the DM, in our setup a SM singlet charged only under the new  $U(1)$ , is introduced. In order to ensure anomaly cancellation, at least one additional state should be present in the dark sector [80].<sup>12</sup> The impact of this additional state, which could, for example, have mass mixing with the DM, is model dependent; its assessment is then beyond the scope of the present paper. We have then implicitly assumed that it is sensibly heavier than the DM and decoupled from the relevant phenomenology.

Along our study we have been agnostic on the generation mechanism of the DM and  $Z'$  masses. A simple possibility would be represented by the vacuum expectation value of a scalar singlet  $S$  spontaneously breaking the  $U(1)'$  symmetry. The  $S$  field can impact the DM phenomenology behaving as an additional mediator (this allows in particular the presence of additional diagrams for the  $\chi\chi \rightarrow Z'Z'$  curing the unitarity violating behavior of the corresponding cross section) and/or final state for DM annihilations [101] and inducing radiatively SI interactions of the DM with nucleons [79]. The results presented in this paper are recovered by assuming that the mass of  $S$  is higher than  $M_{Z'}$ , in order to marginalize its influence in DM processes.<sup>13</sup> We remark, on the other hand, that perturbative unitarity [79] forbids an arbitrary hierarchy between the masses of the DM,  $Z'$  and  $S$  fields.

In UV complete setups, a coupling between the DM and the SM  $Z$  boson would be in general expected. This would be generated by mass mixing between the  $Z$  and the  $Z'$ , due to a nonzero charge of the SM Higgs under the new  $U(1)$  symmetry, or by a kinetic mixing term  $\sin \delta B_{\mu\nu} B^{\mu\nu}$ , which is not forbidden by gauge symmetry. Even if the mixing between  $Z/Z'$  were forbidden at tree level, it would be, in general, expected to arise at the loop level. For example, a kinetic mixing operator would be generated radiatively by SM fermion loops [107], as they are both charged under hypercharge and the new gauge symmetry, while a mass mixing term could be generated by a higher order operator like  $Z'_\mu H^\dagger D^\mu H$ . A  $Z/Z'$  mixing would affect DM DD, still relying on SD interaction, as well as the relic density

<sup>12</sup>This would not be necessary if the DM were a Dirac fermion with only vectorial couplings with the  $Z'$ . As already pointed out, this kind of setup is strongly disfavored by constraints from DM DD.

<sup>13</sup>Invariance under  $U(1)'$  would not forbid a coupling term between  $S$  and the SM Higgs doublet  $H$  of the form  $\lambda_{HS} |H|^2 S^2$  which would be responsible for mass mixing between the two scalars. This would imply a coupling of the DM with the SM Higgs field  $h$ . To prevent this possibility one must further assume the coupling  $\lambda_{HS}$  to be negligible.

through both a modification of the annihilation rate into SM fermions and the addition of annihilation channels into  $WW$  (this is also potentially relevant for the IceCube limits)  $ZZ$ ,  $ZZ'$  and  $Zh$  final states. A quantitative assessment would be again model dependent. The impact of the new interaction is, nevertheless, strongly limited by, for example, Electroweak Precision Tests constraints [108,109]. For simplicity we have then neglected  $Z/Z'$  mixing (assuming a certain degree of fine-tuning) in our study.<sup>14</sup>

As an additional remark, we emphasize that our conclusions rely on thermal production of DM and standard cosmology. Departure from these two assumptions would consequently change the relic density curves and the quantitative assessments based on the latter.

We finally notice that, due to the dominance of the dilepton bounds in the considered setup the other experimental searches play a modest role as far as testing the Majorana nature of the DM in the sequential  $Z'$  portal. Although, direct detection experiments can still be regarded as complementary, because conversely to colliders the observation of signals is tied to the local dark matter density [3].

## V. CONCLUSIONS

We have investigated the Majorana dark matter model in the context of the  $Z'$  portal. The dark matter phenomenology is dictated by gauge interactions which are fixed, since we adopted the sequential  $Z'$  framework, rendering our simplified model predictive. Direct dark matter detection

<sup>14</sup>Along a similar line of reasoning we have also neglected the presence of higher order operators like, for example,  $\frac{1}{\Lambda^2} H^\dagger D_\mu H \bar{\chi} \gamma^\mu \gamma_5 \chi$ .

based on bubble chamber and liquid xenon experiments, and neutrino telescopes observing neutrinos from the Sun, provide complementary tests to this model. LHC searches for *dilepton* and *monojet + missing energy* events provide orthogonal bounds to the parameter space, the former being the stronger one. We computed the relic density curves and outlined the region of parameter space where one can successfully have a Majorana dark matter particle in agreement with data.

We varied the dark matter coupling to the  $Z'$  to assess the impact on the constraints and highlight the importance of complementary probes for dark sectors.

In summary, the Majorana dark matter fermion model via the  $Z'$  portal offers a gripping dark matter phenomenology with exciting implications to neutrino detectors, underground direct detection experiments as well as colliders. Therefore, it should be treated as a benchmark model in dark matter research endeavors.

## ACKNOWLEDGMENTS

The authors thank Carlos Yaguna, Stefan Vogl, Werner Rodejohann, Clarissa Siqueira, Maira Dutra and Alex Dias for discussions. F. S. Q. thanks Yann Mambrini and Abdelhak Djouadi from Orsay-LPT for the hospitality during the final stages of this project. M. D. C. is supported by the International Max Planck Research School (IMPRS) “Precision tests of fundamental symmetries” of the Max Planck Society. The research of A. M. is supported by the ERC Advanced Grant No. 267985 (DaMeSyFla) and by the INFN. A. M. gratefully acknowledges support by the research Grant No. 2012CPPYP7, “Theoretical astroparticle physics,” under the program PRIN 2012 funded by the MIUR. F. S. Q. acknowledges support from MEC and ICTP-SAIFR FAPESP Grant No. 2016/01343-7.

- 
- [1] F. Zwicky, Die Rotverschiebung von extragalaktischen Nebeln, *Helv. Phys. Acta* **6**, 110 (1933).
  - [2] K. A. Olive, in *Proceedings, Theoretical Advanced Study Institute, TASI 2002, Boulder, USA, 2002* (2003), pp. 797–851.
  - [3] G. Arcadi, M. Dutra, P. Ghosh, M. Lindner, Y. Mambrini, M. Pierre, S. Profumo, and F. S. Queiroz, The Waning of the WIMP? A Review of Models, Searches, and Constraints, [arXiv:1703.07364](https://arxiv.org/abs/1703.07364).
  - [4] G. Jungman, M. Kamionkowski, and K. Griest, Supersymmetric dark matter, *Phys. Rep.* **267**, 195 (1996).
  - [5] G. Bertone, D. Hooper, and J. Silk, Particle dark matter: Evidence, candidates and constraints, *Phys. Rep.* **405**, 279 (2005).
  - [6] J. L. Feng, Dark matter candidates from particle physics and methods of detection, *Annu. Rev. Astron. Astrophys.* **48**, 495 (2010).
  - [7] M. Klasen, M. Pohl, and G. Sigl, Indirect and direct search for dark matter, *Prog. Part. Nucl. Phys.* **85**, 1 (2015).
  - [8] T. Marrodan Undagoitia and L. Rauch, Dark matter direct-detection experiments, *J. Phys. G* **43**, 013001 (2016).
  - [9] F. S. Queiroz, W. Rodejohann, and C. E. Yaguna, Is the dark matter particle its own antiparticle?, *Phys. Rev. D* **95**, 095010 (2017).
  - [10] B. J. Kavanagh, F. S. Queiroz, W. Rodejohann, and C. E. Yaguna, Prospects for determining the particle/antiparticle nature of WIMP dark matter with direct detection experiments, *J. High Energy Phys.* **10** (2017) 059.

- [11] J. Abdallah *et al.*, Simplified models for dark matter searches at the LHC, *Phys. Dark Universe* **9–10**, 8 (2015).
- [12] F. Kahlhoefer, Review of LHC dark matter searches, *Int. J. Mod. Phys. A* **32**, 1730006 (2017).
- [13] T. Plehn, Yet another introduction to dark matter, [arXiv:1705.01987](https://arxiv.org/abs/1705.01987).
- [14] F. Aharonian *et al.* (H.E.S.S. Collaboration), H.E.S.S. observations of the Galactic Center Region and their Possible Dark Matter Interpretation, *Phys. Rev. Lett.* **97**, 221102 (2006); Publisher's Note, *Phys. Rev. Lett.* **97**, 249901(E) (2006).
- [15] V. Barger, Y. Gao, W. Y. Keung, D. Marfatia, and G. Shaughnessy, Dark matter and pulsar signals for Fermi LAT, PAMELA, ATIC, HESS and WMAP data, *Phys. Lett. B* **678**, 283 (2009).
- [16] K. N. Abazajian and J. P. Harding, Constraints on WIMP and Sommerfeld-enhanced dark matter annihilation from HESS observations of the Galactic center, *J. Cosmol. Astropart. Phys.* **01** (2012) 041.
- [17] J. A. R. Cembranos, V. Gammaldi, and A. L. Maroto, Possible dark matter origin of the gamma ray emission from the Galactic center observed by HESS, *Phys. Rev. D* **86**, 103506 (2012).
- [18] M. Ackermann *et al.* (Fermi-LAT Collaboration), Updated search for spectral lines from galactic dark matter interactions with pass 8 data from the Fermi Large Area Telescope, *Phys. Rev. D* **91**, 122002 (2015).
- [19] H. Abdallah *et al.* (H.E.S.S. Collaboration), Search for Dark Matter Annihilations Towards the Inner Galactic Halo from 10 Years of Observations with H.E.S.S., *Phys. Rev. Lett.* **117**, 111301 (2016).
- [20] E. Charles *et al.* (Fermi-LAT Collaboration), Sensitivity projections for dark matter searches with the Fermi Large Area Telescope, *Phys. Rep.* **636**, 1 (2016).
- [21] M. L. Ahnen *et al.* (Fermi-LAT, MAGIC Collaboration), Limits to dark matter annihilation cross section from a combined analysis of MAGIC and Fermi-LAT observations of dwarf satellite galaxies, *J. Cosmol. Astropart. Phys.* **02** (2016) 039.
- [22] G. Beck and S. Colafrancesco, Multifrequency search for dark matter: The role of HESS, CTA, and SKA, *Proc. Sci., HEASA20162017* (2017) 010 [[arXiv:1704.08029](https://arxiv.org/abs/1704.08029)].
- [23] A. Albert *et al.* (DES, Fermi-LAT Collaboration), Searching for dark matter annihilation in recently discovered Milky Way satellites with Fermi-LAT, *Astrophys. J.* **834**, 110 (2017).
- [24] M. Ackermann *et al.* (Fermi-LAT Collaboration), The Fermi Galactic center GeV excess and implications for dark matter, *Astrophys. J.* **840**, 43 (2017).
- [25] T. Bringmann, M. Doro, and M. Fornasa, Dark matter signals from Draco and Willman 1: Prospects for MAGIC II and CTA, *J. Cosmol. Astropart. Phys.* **01** (2009) 016.
- [26] M. Pierre, J. M. Siegal-Gaskins, and P. Scott, Sensitivity of CTA to dark matter signals from the Galactic center, *J. Cosmol. Astropart. Phys.* **06** (2014) 024; Erratum, *J. Cosmol. Astropart. Phys.* **10** (2014) E01.
- [27] H. Silverwood, C. Weniger, P. Scott, and G. Bertone, A realistic assessment of the CTA sensitivity to dark matter annihilation, *J. Cosmol. Astropart. Phys.* **03** (2015) 055.
- [28] A. Ibarra, A. S. Lamperstorfer, S. Lopez-Gehler, M. Pato, and G. Bertone, On the sensitivity of CTA to gamma-ray boxes from multi-TeV dark matter, *J. Cosmol. Astropart. Phys.* **09** (2015) 048; Erratum, *J. Cosmol. Astropart. Phys.* **06** (2016) E02.
- [29] L. Roszkowski, E. M. Sessolo, S. Trojanowski, and A. J. Williams, Reconstructing WIMP properties through an interplay of signal measurements in direct detection, Fermi-LAT, and CTA searches for dark matter, *J. Cosmol. Astropart. Phys.* **08** (2016) 033.
- [30] C. Balazs, J. Conrad, B. Farmer, T. Jacques, T. Li, M. Meyer, F. S. Queiroz, and M. A. Sánchez-Conde, Sensitivity of the Cherenkov Telescope Array to the detection of a dark matter signal in comparison to direct detection and collider experiments, *Phys. Rev. D* **96**, 083002 (2017).
- [31] T. Bringmann, X. Huang, A. Ibarra, S. Vogl, and C. Weniger, Fermi LAT search for internal Bremsstrahlung signatures from dark matter annihilation, *J. Cosmol. Astropart. Phys.* **07** (2012) 054.
- [32] T. Bringmann and C. Weniger, Gamma-ray signals from dark matter: Concepts, status, and prospects, *Phys. Dark Universe* **1**, 194 (2012).
- [33] L. Bergstrom, J. Edsjo, and P. Gondolo, Indirect neutralino detection rates in neutrino telescopes, *Phys. Rev. D* **55**, 1765 (1997).
- [34] P. Gondolo, J. Edsjo, P. Ullio, L. Bergstrom, M. Schelke, and E. A. Baltz, DarkSUSY: Computing supersymmetric dark matter properties numerically, *J. Cosmol. Astropart. Phys.* **07** (2004) 008.
- [35] M. Blennow, J. Edsjo, and T. Ohlsson, Neutrinos from WIMP annihilations using a full three-flavor Monte Carlo, *J. Cosmol. Astropart. Phys.* **01** (2008) 021.
- [36] G. Wikstrom and J. Edsjo, Limits on the WIMP-nucleon scattering cross section from neutrino telescopes, *J. Cosmol. Astropart. Phys.* **04** (2009) 009.
- [37] M. Lattanzi, R. A. Lineros, and M. Taoso, Connecting neutrino physics with dark matter, *New J. Phys.* **16**, 125012 (2014).
- [38] C. E. Yaguna, Isospin-violating dark matter in the light of recent data, *Phys. Rev. D* **95**, 055015 (2017).
- [39] A. Alves, S. Profumo, and F. S. Queiroz, The dark  $Z'$  portal: Direct, indirect, and collider searches, *J. High Energy Phys.* **04** (2014) 063.
- [40] C. Kouvaris, Dark Majorana particles from the minimal walking technicolor, *Phys. Rev. D* **76**, 015011 (2007).
- [41] K. Belotsky, M. Khlopov, and C. Kouvaris, Muon flux limits for Majorana dark matter from strong coupling theories, *Phys. Rev. D* **79**, 083520 (2009).
- [42] J. Goodman, M. Ibe, A. Rajaraman, W. Shepherd, T. M. P. Tait, and H.-B. Yu, Constraints on light Majorana dark matter from colliders, *Phys. Lett. B* **695**, 185 (2011).
- [43] M. Garny, A. Ibarra, and S. Vogl, Signatures of Majorana dark matter with t-channel mediators, *Int. J. Mod. Phys. D* **24**, 1530019 (2015).
- [44] P. Ciafaloni, M. Cirelli, D. Comelli, A. De Simone, A. Riotto, and A. Urbano, On the importance of electroweak corrections for Majorana dark matter indirect detection, *J. Cosmol. Astropart. Phys.* **06** (2011) 018.

- [45] P. Ciafaloni, M. Cirelli, D. Comelli, A. De Simone, A. Riotto, and A. Urbano, Initial state radiation in Majorana dark matter annihilations, *J. Cosmol. Astropart. Phys.* **10** (2011) 034.
- [46] M. Duerr, P. Fileviez Perez, and J. Smirnov, Gamma lines from Majorana dark matter, *Phys. Rev. D* **93**, 023509 (2016).
- [47] J. Heisig, M. Krämer, M. Pellen, and C. Wiebusch, Constraints on Majorana dark matter from the LHC and IceCube, *Phys. Rev. D* **93**, 055029 (2016).
- [48] M. Dutra, C. A. de S. Pires, and P. S. Rodrigues da Silva, Majorana dark matter through a narrow Higgs portal, *J. High Energy Phys.* **09** (2015) 147.
- [49] L. A. Anchordoqui, V. Barger, H. Goldberg, X. Huang, D. Marfatia, L. H. M. da Silva, and T. J. Weiler, Majorana dark matter through the Higgs portal under the vacuum stability lamppost, *Phys. Rev. D* **92**, 063504 (2015).
- [50] C.-K. Chua and G.-G. Wong, Study of Majorana Fermionic dark matter, *Phys. Rev. D* **94**, 035002 (2016).
- [51] D. Hooper,  $Z'$  mediated dark matter models for the Galactic center gamma-ray excess, *Phys. Rev. D* **91**, 035025 (2015).
- [52] T. Nomura, H. Okada, and Y. Orikasa, Radiative seesaw model with degenerate Majorana dark matter, *Phys. Rev. D* **93**, 113008 (2016).
- [53] W. Chao, H.-k. Guo, and Y. Zhang, Majorana dark matter with  $B + L$  gauge symmetry, *J. High Energy Phys.* **04** (2017) 034.
- [54] C. A. de S. Pires, P. S. Rodrigues da Silva, A. C. O. Santos, and C. Siqueira, Higgs mass and right-handed sneutrino WIMP in a supersymmetric  $3 - 3 - 1$  model, *Phys. Rev. D* **94**, 055014 (2016).
- [55] S. Matsumoto, S. Mukhopadhyay, and Y.-L. S. Tsai, Effective theory of WIMP dark matter supplemented by simplified models: Singletlike Majorana fermion case, *Phys. Rev. D* **94**, 065034 (2016).
- [56] J. D. Ruiz-Alvarez, C. A. de S. Pires, F. S. Queiroz, D. Restrepo, and P. S. Rodrigues da Silva, On the connection of gamma rays, dark matter and Higgs searches at the LHC, *Phys. Rev. D* **86**, 075011 (2012).
- [57] S. Profumo and F. S. Queiroz, Constraining the  $Z'$  mass in 331 models using direct dark matter detection, *Eur. Phys. J. C* **74**, 2960 (2014).
- [58] A. Alves, A. Berlin, S. Profumo, and F. S. Queiroz, Dark matter complementarity and the  $Z'$  portal, *Phys. Rev. D* **92**, 083004 (2015).
- [59] A. Alves, A. Berlin, S. Profumo, and F. S. Queiroz, Dirac-fermionic dark matter in  $U(1)_X$  models, *J. High Energy Phys.* **10** (2015) 076.
- [60] M. Duerr, P. Fileviez Perez, and J. Smirnov, Simplified Dirac dark matter models and gamma-ray lines, *Phys. Rev. D* **92**, 083521 (2015).
- [61] B. Allanach, F. S. Queiroz, A. Strumia, and S. Sun,  $Z$  models for the LHCb and  $g - 2$  muon anomalies, *Phys. Rev. D* **93**, 055045 (2016).
- [62] M. Lindner, F. S. Queiroz, and W. Rodejohann, Dilepton bounds on left-right symmetry at the LHC run II and neutrinoless double beta decay, *Phys. Lett. B* **762**, 190 (2016).
- [63] M. Klasen, F. Lyonnet, and F. S. Queiroz, NLO+NLL collider bounds, Dirac fermion and scalar dark matter in the B-L model, *Eur. Phys. J. C* **77**, 348 (2017).
- [64] W. Altmannshofer, S. Gori, S. Profumo, and F. S. Queiroz, Explaining dark matter and B decay anomalies with an  $L_\mu - L_\tau$  model, *J. High Energy Phys.* **12** (2016) 106.
- [65] A. Alves, G. Arcadi, P. V. Dong, L. Duarte, F. S. Queiroz, and J. W. F. Valle, R-parity as a residual gauge symmetry: Probing a theory of cosmological dark matter, *Phys. Lett. B* **772**, 825 (2017).
- [66] A. Alves, G. Arcadi, Y. Mambrini, S. Profumo, and F. S. Queiroz, Augury of darkness: The low-mass dark Z portal, *J. High Energy Phys.* **04** (2017) 164.
- [67] G. Arcadi, M. Lindner, Y. Mambrini, M. Pierre, and F. S. Queiroz, GUT models at current and future hadron colliders and implications to dark matter searches, *Phys. Lett. B* **771**, 508 (2017).
- [68] M. D. Campos, D. Cogollo, M. Lindner, T. Melo, F. S. Queiroz, and W. Rodejohann, Neutrino masses and absence of flavor changing interactions in the 2HDM from gauge principles, *J. High Energy Phys.* **08** (2017) 092.
- [69] J. K. Mizukoshi, C. A. de S. Pires, F. S. Queiroz, and P. S. Rodrigues da Silva, WIMPs in a 3-3-1 model with heavy sterile neutrinos, *Phys. Rev. D* **83**, 065024 (2011).
- [70] C. Kelso, C. A. de S. Pires, S. Profumo, F. S. Queiroz, and P. S. Rodrigues da Silva, A 331 WIMPY dark radiation model, *Eur. Phys. J. C* **74**, 2797 (2014).
- [71] J. Heeck, M. Holthausen, W. Rodejohann, and Y. Shimizu, Higgs  $\rightarrow \mu\tau$  in Abelian and non-Abelian flavor symmetry models, *Nucl. Phys.* **B896**, 281 (2015).
- [72] W. Rodejohann and C. E. Yaguna, Scalar dark matter in the B-L model, *J. Cosmol. Astropart. Phys.* **12** (2015) 032.
- [73] S. Patra, F. S. Queiroz, and W. Rodejohann, Stringent dilepton bounds on left-right models using LHC data, *Phys. Lett. B* **752**, 186 (2016).
- [74] S. Patra, W. Rodejohann, and C. E. Yaguna, A new B-L model without right-handed neutrinos, *J. High Energy Phys.* **09** (2016) 076.
- [75] M. Lindner, F. S. Queiroz, W. Rodejohann, and C. E. Yaguna, Left-right symmetry and lepton number violation at the Large Hadron Electron Collider, *J. High Energy Phys.* **06** (2016) 140.
- [76] M. Carena, A. Daleo, B. A. Dobrescu, and T. M. P. Tait,  $Z'$  gauge bosons at the Tevatron, *Phys. Rev. D* **70**, 093009 (2004).
- [77] T. Appelquist, B. A. Dobrescu, and A. R. Hopper, Non-exotic neutral gauge bosons, *Phys. Rev. D* **68**, 035012 (2003).
- [78] A. Albert *et al.*, Recommendations of the LHC dark matter Working Group: Comparing LHC searches for heavy mediators of dark matter production in visible and invisible decay channels, [arXiv:1703.05703](https://arxiv.org/abs/1703.05703).
- [79] F. Kahlhoefer, K. Schmidt-Hoberg, T. Schwetz, and S. Vogl, Implications of unitarity and gauge invariance for simplified dark matter models, *J. High Energy Phys.* **02** (2016) 016.
- [80] J. Ellis, M. Fairbairn, and P. Tunney, Anomaly-free dark matter models are not so simple, *J. High Energy Phys.* **08** (2017) 053.

- [81] P. A. R. Ade *et al.* (Planck Collaboration), Planck 2015 results. XIII. Cosmological parameters, *Astron. Astrophys.* **594**, A13 (2016).
- [82] D. Barducci, G. Belanger, J. Bernon, F. Boudjema, J. Da Silva, S. Kraml, U. Laa, and A. Pukhov, Collider limits on new physics within micrOMEGAs, *Comput. Phys. Commun.* **222**, 327 (2018).
- [83] C. Amole *et al.* (PICO Collaboration), Dark Matter Search Results from the PICO-60  $C_3F_8$  Bubble Chamber, *Phys. Rev. Lett.* **118**, 251301 (2017).
- [84] A. Ibarra, M. Totzauer, and S. Wild, Higher order dark matter annihilations in the Sun and implications for IceCube, *J. Cosmol. Astropart. Phys.* **04** (2014) 012.
- [85] M. G. Aartsen *et al.* (IceCube Collaboration), Search for annihilating dark matter in the Sun with 3 years of IceCube data, *Eur. Phys. J. C* **77**, 146 (2017).
- [86] D. S. Akerib *et al.* (LUX Collaboration), Improved Limits on Scattering of Weakly Interacting Massive Particles from Reanalysis of 2013 LUX Data, *Phys. Rev. Lett.* **116**, 161301 (2016).
- [87] C. Fu *et al.* (PandaX-II Collaboration), Spin-Dependent Weakly-Interacting-Massive-Particle-Nucleon Cross Section Limits from First Data of PandaX-II Experiment, *Phys. Rev. Lett.* **118**, 071301 (2017).
- [88] Y. Yang (PandaX-II Collaboration), Search for dark matter from the first data of the PandaX-II experiment, *Proc. Sci., ICHEP20162016* (2016) 224 [arXiv:1612.01223].
- [89] A. Tan *et al.* (PandaX-II Collaboration), Dark Matter Results from First 98.7 Days of Data from the PandaX-II Experiment, *Phys. Rev. Lett.* **117**, 121303 (2016).
- [90] E. Aprile *et al.* (XENON100 Collaboration), XENON100 dark matter results from a combination of 477 live days, *Phys. Rev. D* **94**, 122001 (2016).
- [91] D. S. Akerib *et al.* (LUX Collaboration), Limits on Spin-Dependent WIMP-Nucleon Cross Section Obtained from the Complete LUX Exposure, *Phys. Rev. Lett.* **118**, 251302 (2017).
- [92] E. Aprile *et al.* (XENON100 Collaboration), Limits on Spin-Dependent WIMP-Nucleon Cross Sections from 225 Live Days of XENON100 data, *Phys. Rev. Lett.* **111**, 021301 (2013).
- [93] G. B. Gelmini and P. Gondolo, Neutralino with the right cold dark matter abundance in (almost) any supersymmetric model, *Phys. Rev. D* **74**, 023510 (2006).
- [94] G. Gelmini, P. Gondolo, A. Soldatenko, and C. E. Yaguna, The effect of a late decaying scalar on the neutralino relic density, *Phys. Rev. D* **74**, 083514 (2006).
- [95] G. Arcadi and P. Ullio, Accurate estimate of the relic density and the kinetic decoupling in nonthermal dark matter models, *Phys. Rev. D* **84**, 043520 (2011).
- [96] M. Aaboud *et al.* (ATLAS Collaboration), Search for new high-mass phenomena in the dilepton final state using  $36.1 \text{ fb}^{-1}$  of proton-proton collision data at  $\sqrt{s} = 13 \text{ TeV}$  with the ATLAS detector, *J. High Energy Phys.* **10** (2017) 182.
- [97] E. Accomando, J. Fiaschi, F. Hautmann, S. Moretti, and C. H. Shepherd-Themistocleous, The effect of real and virtual photons in the dilepton channel at the LHC, *Phys. Lett. B* **770**, 1 (2017).
- [98] G. Arcadi, Y. Mambrini, M. H. G. Tytgat, and B. Zaldivar, Invisible  $Z'$  and dark matter: LHC vs LUX constraints, *J. High Energy Phys.* **03** (2014) 134.
- [99] J. Shu, Unitarity bounds for new physics from axial coupling at the LHC, *Phys. Rev. D* **78**, 096004 (2008).
- [100] M. Drees and M. M. Nojiri, The neutralino relic density in minimal  $N = 1$  supergravity, *Phys. Rev. D* **47**, 376 (1993).
- [101] M. Duerr, F. Kahlhoefer, K. Schmidt-Hoberg, T. Schwetz, and S. Vogl, How to save the WIMP: Global analysis of a dark matter model with two s-channel mediators, *J. High Energy Phys.* **09** (2016) 042.
- [102] N. F. Bell, Y. Cai, and R. K. Leane, Impact of mass generation for spin-1 mediator simplified models, *J. Cosmol. Astropart. Phys.* **01** (2017) 039.
- [103] Y. Cui and F. D'Eramo, On the completeness of vector portal theories: New insights into the dark sector and its interplay with Higgs physics, *Phys. Rev. D* **96**, 095006 (2017).
- [104] P. Langacker, The physics of heavy  $Z'$  gauge bosons, *Rev. Mod. Phys.* **81**, 1199 (2009).
- [105] A. M. Sirunyan *et al.* (CMS Collaboration), Search for dijet resonances in proton-proton collisions at  $\sqrt{s} = 13 \text{ TeV}$  and constraints on dark matter and other models, *Phys. Lett. B* **769**, 520 (2017); Corrigendum, *Phys. Lett. B* **772**, 882(E) (2017).
- [106] M. Aaboud *et al.* (ATLAS Collaboration), Search for new phenomena in dijet events using  $37 \text{ fb}^{-1}$  of  $pp$  collision data collected at  $\sqrt{s} = 13 \text{ TeV}$  with the ATLAS detector, *Phys. Rev. D* **96**, 052004 (2017).
- [107] B. Holdom, Two  $U(1)$ 's and epsilon charge shifts, *Phys. Lett.* **166B**, 196 (1986).
- [108] J. Kumar and J. D. Wells, CERN LHC and ILC probes of hidden-sector gauge bosons, *Phys. Rev. D* **74**, 115017 (2006).
- [109] E. J. Chun, J.-C. Park, and S. Scopel, Dark matter and a new gauge boson through kinetic mixing, *J. High Energy Phys.* **02** (2011) 100.